# Diffusion study in tailored gratings recorded in photopolymer glass with high refractive index species

Óscar Martínez-Matos, María L. Calvo, José A. Rodrigo, Pavel Cheben, and Francisco del Monte

Citation: Applied Physics Letters **91**, 141115 (2007); doi: 10.1063/1.2794792
View online: http://dx.doi.org/10.1063/1.2794792
View Table of Contents: http://scitation.aip.org/content/aip/journal/apl/91/14?ver=pdfcov
Published by the AIP Publishing

# Diffusion study in tailored gratings recorded in photopolymer glass with high refractive index species

Óscar Martínez-Matos,[a] María L. Calvo, and José A. Rodrigo
*Departamento de Óptica, Facultad de Ciencias Físicas, Universidad Complutense de Madrid, 28040 Madrid, Spain*

Pavel Cheben
*Institute for Microstructural Sciences, National Research Council of Canada, K1A 0R6 Ottawa, Canada*

Francisco del Monte
*Instituto de Ciencia de Materiales, Consejo Superior de Investigaciones Científicas (CSIC), 28049 Madrid, Spain*

(Received 6 June 2007; accepted 17 September 2007; published online 3 October 2007)

We report results on the temporal evolution of the diffraction efficiency of volume holographic gratings recorded in a photopolymer glass incorporating Zr-based high refractive index species (HRIS) at molecular level. We record high spatial frequency gratings in this material with diffraction efficiencies near 100%. A two-component diffusion model is introduced for the evolution of refractive index modulation in darkness. Diffusion parameters for the Zr-based HRIS and monomer components have been determined. Codirectional diffusion of both components is demonstrated. The results show the feasibility for tailoring in this photomaterial holographic gratings with high diffraction efficiency over a wide range of spatial frequencies. © *2007 American Institute of Physics*. [DOI: 10.1063/1.2794792]

A sol-gel volume holographic glass with Zr-based high refractive index species incorporated at a molecular level has been recently developed[1] suitable for recording holographic gratings with high performance. Sol-gel technique has been widely applied in materials science and nanotechnology, including holography since a volume holographic grating was recorded in a sol-gel glass in 1996.[2] The material[1] under study in this paper is a modified composition of a highly efficient photopolymerizable sol-gel glass synthesized earlier by Cheben and Calvo,[3] wherein the modification includes the Zr-based modulation enhancing species. The use of $Zr(O^iPr)_4$ requires its hydrolysis kinetics to be slowed down through the formation of a complex with a chelating agent, namely, methacrylic acid (MA). The main characteristic of the MA:Zr-based photomaterial is the diffusion enhancement upon inhomogeneous illumination, yielding an increased dynamic range, along with low coherent and incoherent scattering noise and dimension stability. These requirements are particularly important for holographic optical operations and data storage since the latter demands highly optimized photomaterials. Furthermore, a type of overmodulation effect, the optical Pendellösung effect, predicted theoretically in 1993,[4,5] was reported in the visible domain[6] using this material.[1]

In this paper, we report results on the temporal evolution of the diffraction efficiency of a nonactinic He–Ne laser probe beam during and after recording exposition and consider these results for studying the diffusion process of two polymerizable and diffusible species in our sol-gel matrix.[1] We have recorded the transmission volume holographic gratings by two mutually coherent *s*-polarized collimated writing beams at different angles using a frequency-doubled Nd:yttrium aluminum garnet laser with a wavelength of 532 nm. Samples were prepared with various thickness ranges following the synthesis reported in detail by del Monte *et al.*[1] For grating recording, the samples were positioned on a rotation stage with an angular accuracy of 0.001° to allow Bragg angle tuning of the probe beam. Zero and first diffraction orders were measured using a dual power meter. The evaluation and further optimization of the recorded holographic gratings to achieve a maximum efficiency were performed by diffraction efficiency measurements under Bragg condition. To have a real data of the first-order diffracted energy, one can consider the initial energy of the reading beam, 200 $\mu W/cm^2$, for the three studied samples. The temporal evolution of the grating efficiency was measured in real time. Figures 1(a)–1(c) show the results obtained for three samples, with spatial frequencies of 556, 1135, and 2031 lines/mm, respectively. Gray rectangular regions in Figs. 1(a)–1(c) represent time exposure duration followed by the dark diffusion transient. Right column, Figs. 1(d)–1(f) show the angular selectivity of each grating where dots represent experimental results and solid lines the fits to Kogelnik's coupled-wave theory for volume holographic gratings.[7] Relevant physical parameters of the holographic recording process and the grating, including sample thickness ($T$), grating spatial frequency, Bragg angle ($\theta_B$), refractive index modulation ($\Delta n$), and $Q$ parameter,[7] are also provided in Fig. 1. The exposure time was chosen in all samples such that the maximum diffraction efficiency is obtained. Longer exposure intervals result in the overmodulation effect and a corresponding decrease in the reconstruction fidelity (Pendellösung effect)[6] and diffraction efficiency.

In all the studied cases, we found excellent agreement between the experimental and the theoretical angular selectivity results, including the three first secondary maxima and minima of the angular selectivity curves. This attests to the high quality and homogeneity of the gratings, with no notice-

[a]Author to whom correspondence should be addressed. Electronic mail: ommatos@fis.ucm.es



 

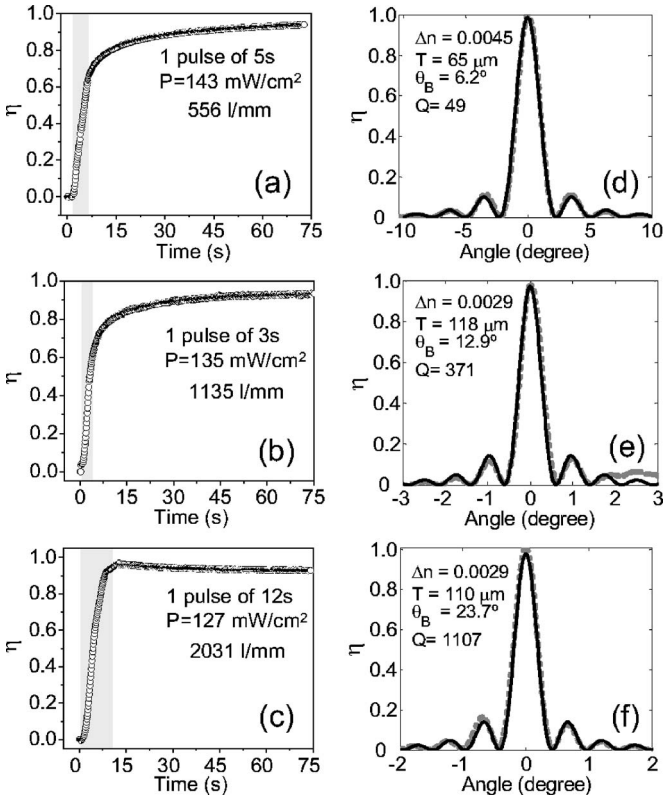


FIG. 1. Diffraction efficiency measurements of a He–Ne laser probe for three samples with spatial frequencies of 556, 1135, and 2031 lines/mm. Left column [(a)–(c)] show temporal evolution of grating efficiency under Bragg condition during and after holographic exposure. The gray region in (a)–(c) indicates the exposure time interval, with the recording beams present. Right column [(d)–(f)] show the experimental results for the angular selectivity associated with each grating (dots) and the fits to Kogelnik's theory (solid lines). Thickness of the grating ($T$), recording time, writing beam irradiance, Klein-Cook parameter $Q$, incident angle of the reading beam inside the material, and $\Delta n$ corresponding to ~100% efficiency are also shown.

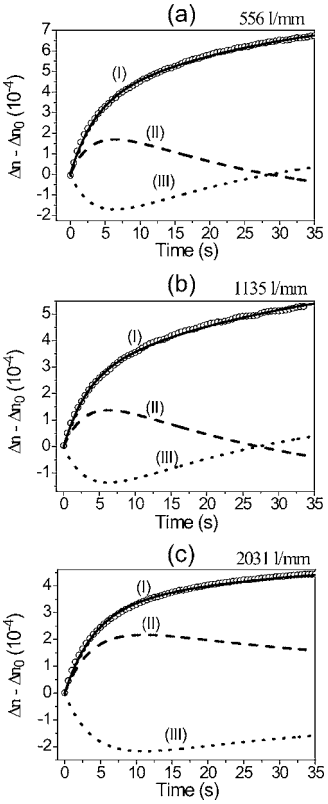


FIG. 2. Evolution of refractive index modulation in darkness. 6 s exposure of 130 mW/cm$^2$ irradiance for three gratings with spatial frequencies of 556 (a), 1135 (b), and 2031 lines/mm (c). Dots represent the experimental results and solid, dash, and dot lines are fits using expression (1) for the codirectional (I) and counterdiffusion (II and III), respectively. The parameters have been used as in Table I with the following signs: $(c_M, c_{Zr}, \tau_M, \tau_{Zr})$, $(c_M, -c_{Zr}, \tau_M, \tau_{Zr})$, and $(-c_M, c_{Zr}, \tau_M, \tau_{Zr})$ for curves (I), (II), and (III), respectively.

able gradient in $\Delta n$ throughout the depth of the samples, even for samples with thicknesses over 100 $\mu$m.

In Figs. 1(a)–1(c), we can distinguish two regimes of grating formation for the studied spatial frequency range. Nearly linear part corresponds to polymerization and diffusion of monomer and MA:Zr species during the exposure time (gray rectangle), followed by a nonlinear part corresponding to dark grating formation involving diffusion mechanism of the two species in the absence of the photoinitiation process. We will study this second stage by a two-component diffusion model.

In the recording process, the light interference pattern formed by coherent superposition of two plane waves initiates photopolymerization in the illuminated regions. The polymerization results in a monomer concentration gradient and corresponding monomer diffusion, as suggested by Colburn and Haines.[8] The monomer dark diffusion transient was studied by Piazzolla and Jenkins[9] for a one-component free monomer diffusion model. They demonstrated that the variation of the recorded grating modulation $[\Delta n(t)]$ during dark diffusion transient follows an exponential law. For our material, the model can be extended to include the contribution of two diffusible components, namely, the acrylic monomer 2-phenoxyethyl acrylate (POEA) and MA:Zr complex, according to the following equation:

$$\Delta n(t) - \Delta n_0(t_0) = \pm c_M[1 - \exp(-t/\tau_M)] \pm c_{Zr}[1 - \exp(-t/\tau_{Zr})], \quad (1)$$

where $\Delta n(t_0)$ is the refractive index modulation immediately after exposure time of duration $t_0$, $c_M$ and $c_{Zr}$ are the contributions of the first harmonic term of the free monomer concentration and of the MA:Zr complex, respectively, and $\tau_M$ and $\tau_{Zr}$ are the diffusion times of monomer and the MA:Zr complex, respectively. The positive and negative signs in Eq. (1) accounts for two possible diffusion mechanisms, namely, equal signs for both components corresponding to in-phase grating formation and the opposite signs indicating two gratings dephased $\pi$ radians. The later, named counterdiffusion, has been recently reported in nanoparticle-dispersed photopolymers.[10–12] From Eq. (1), it is observed that the counterdiffusion produces a decrease in the index modulation, which is undesirable in holographic materials when large dynamic range is aimed for.

Figure 2 shows the temporal evolution in darkness of $\Delta n(t)$ for gratings with spatial frequencies of 556 (a), 1135 (b) and 2031 lines/mm (c). The samples were illuminated for duration of 6 s with 130 mW/cm$^2$ irradiance. The origin of the curves is referenced to zero by subtracting the value of the refractive index modulation $[\Delta n(t_0)]$ measured immediately upon the pulse duration $t_0$=6 s. Circles represent experimental results and solid, dash, and dot lines are biexponential fits to a two diffusion component model by means of Eq. (1) for the codirectional (I) and two counterdiffusion

TABLE I. Parameters used to fit experimental results displayed in Fig. 2 for codirectional diffusion.

| Spatial frequency (lines/mm) | $c_M$ $(10^{-4})$ | $c_{Zr}$ $(10^{-4})$ | $\tau_M$ (s) | $\tau_{Zr}$ (s) |
|---|---|---|---|---|
| 556 | 3.2 | 4.9 | 3.3 | 27.0 |
| 1135 | 2.5 | 4.3 | 3.2 | 31.2 |
| 2031 | 3.0 | 2.0 | 4.0 | 28.6 |

(II, III) cases, respectively. An excellent fit is observed for the codirectional diffusion [positive signs in Eq. (1)]. The parameters used in this fit for gratings of different spatial frequencies are summarized in Table I.

We find that there is an order of magnitude difference between diffusion times for the two components. As one may expect, it is observed a longer $\tau$ to the heavier specie (MA:Zr complex $\tau_{Zr}$) and a shorter $\tau$ for the lighter specie (monomer $\tau_M$). Similar values of $\tau_M$ have been found for the DuPont HRF-150-38 photopolymer[9] in which diffusion time range was 0.5–2 s. On the other hand, we observe in Table I similar contributions of each of the individual species to the index modulation value given by the parameters $c_M$ and $c_{Zr}$. It is also observed that if MA:Zr complex species are excluded from the photopolymerizable glass ($c_{Zr}=0$), maximum $\Delta n$ value would reach approximately one-half of the maximum value for MA:Zr-based photomaterial, in accordance with our previous experimental results.[1]

Moreover, no set of physical parameters can fit experimental data satisfactory for counterdiffusion. Figure 2 shows the evolution of refractive index modulation for two possible cases of counterdiffusion using the parameters as in Table I but with correspondingly modified signs. In Fig. 2, curve II was obtained for $c_M$, $-c_{Zr}$, $\tau_M$, and $\tau_{Zr}$, while curve III for $-c_M$, $c_{Zr}$, $\tau_M$, and $\tau_{Zr}$. For counterdiffusion II (III), index modulation reaches a maximum (minimum) and then evolves with decreasing (increasing) $\Delta n(t)$. This phenomenon was not observed in our experimental results, ruling out a significance of counterdiffusion processes in our glass.

We may mention that the considered diffusion model does not formally include two aspects reported by Zhao and Mouroulis[13] and Sheridan *et al.*[14] The first aspect is the finite size of the polymer chains, which influences among other material characteristics the values of parameters $c_M$, $c_{Zr}$, $\tau_M$, and $\tau_{Zr}$. However, our results (Table I) account for this effect indirectly since the corresponding parameter values found here were obtained from experimental results, as shown in Fig. 2. The second aspect is the nonlinearity in the material holographic response and the holographic *reciprocity failure*. The nonlinear response concerns in the distortion of the grating that can be represented by the first and higher harmonics of the grating. The amplitude of the first-order grating is affected by the formation of higher order gratings due to the nonlinearity of the fringe formation process.[13] These effects can be reduced by staggering the exposure over time.[14] Experiments in present work were performed in linear regime. The gratings were allowed to evolve time long enough and the monomer to diffuse and to mimic the interference pattern.

In conclusion, we have studied the dynamics of the grating formation in a photopolymer glass in which high refractive index species have been incorporated at a molecular level for a spatial frequency range of ~500–2000 lines/mm. By means of a simple model, we studied the diffusion of two components, namely, the POEA monomer and the MA:Zr complex, in darkness after the recording exposure. Both species contribute with similar weights ($c_M$ and $c_{Zr}$) to grating formation with an order magnitude difference in the respective diffusion times. We also demonstrated that counterdiffusion does not take place in our modified photopolymerizable glass. The feasibility of tailoring in this photomaterial holographic gratings with high quality diffraction efficiencies close to 100% was demonstrated for a large range of spatial frequencies.

The financial support from the Spanish Ministry of Education and Science under Project No. TEC2005-02180 is gratefully acknowledged.

[1] F. del Monte, O. Martínez Matos, J. A. Rodrigo, M. L. Calvo, and P. Cheben, Adv. Mater. (Weinheim, Ger.) **18**, 2014 (2006).
[2] P. Cheben, T. Belenguer, A. Núñez, F. del Monte, and D. Levy, Opt. Lett. **21**, 1857 (1996).
[3] P. Cheben and M. L. Calvo, Appl. Phys. Lett. **78**, 1490 (2001).
[4] P. Cheben and M. L. Calvo, J. Opt. Soc. Am. A **10**, 2573 (1993).
[5] P. Cheben and M. L. Calvo, J. Opt. Soc. Am. A **13**, 131 (1996).
[6] M. L. Calvo, P. Cheben, O. Martínez Matos, J. A. Rodrigo, and F. del Monte, Phys. Rev. Lett. **97**, 084801 (2006).
[7] H. Kogelnik, Bell Syst. Tech. J. **48**, 2909 (1969).
[8] W. S. Colburn and K. A. Haines, Appl. Opt. **10**, 1636 (1971).
[9] S. Piazzolla and B. K. Jenkins, J. Opt. Soc. Am. B **17**, 1147 (2000).
[10] Y. Tomita, N. Suzuki, and K. Chikama, Opt. Lett. **30**, 839 (2005).
[11] Y. Tomita, K. Furushima, K. Ochi, K. Ishizu, A. Tanaka, M. Ozawa, M. Hidaka, and K. Chikama, Appl. Phys. Lett. **88**, 071103 (2006).
[12] N. Suzuki and Y. Tomita, Appl. Phys. Lett. **88**, 011105 (2006).
[13] G. Zhao and P. Mouroulis, J. Mod. Opt. **41**, 1929 (1994).
[14] J. T. Sheridan, F. T. O'Neill, and J. V. Kelly, J. Opt. Soc. Am. B **21**, 1443 (2004).